

Characterization of copper powder particles obtained by electrodeposition as function of different current densities

V. M. Maksimović · Lj. J. Pavlović ·
M. G. Pavlović · M. V. Tomić

Received: 9 February 2009 / Accepted: 8 June 2009 / Published online: 26 June 2009
© Springer Science+Business Media B.V. 2009

Abstract Technological properties of powders depend on their granulometry and morphology. Very often one method is inadequate for characterization of powder particles. This article studied different methods intended for clear definition of the copper powder granulometric and morphological properties. Quantitative microstructural analysis, sieve analysis, and XRD analysis of copper powder as well as scanning electron microscopy analysis of the copper powder particles were performed. It was determined that selected stereological parameters, such as area, perimeter, and shape factor (roundness) show a linear decreasing dependence of current density, while the morphology was changed from massive to branched 3D dendrites. XRD analysis indicated that the crystallite sizes shows a linearly increasing dependence on current density. The shape factor could be a useful parameter for description of powder morphologies deposited by different regimes.

Keywords Copper powder particles · Morphology · Granulometry · Stereology · Shape factor

1 Introduction

Recently, powder metallurgy has rapidly grown with regard to both the variety and the quantity of metal powders produced. Over the last 10 years, a double-digit increase in metal powder production was not unexpected [1]. Almost all the materials can be obtained as a powder, but the method selected for production of powder depends on the specific material properties. The four main categories of fabrication techniques are based on mechanical comminuting, chemical reaction, electrolytic deposition, and liquid metal atomization [2].

The metal powder obtained by electrodeposition represents a disperse deposit, removed from the electrode by tapping or in a similar way [3, 4], which consists of particles of various forms and sizes. The electrolytic powder production method usually yields products of high purity, which can be easily pressed and sintered. Besides, in recent years, it has been shown that by different electrolysis regimes, it is possible, not only to obtain powders with a wide range of properties, but also to predict the decisive characteristics of powders, which are very important for powder quality and for the appropriate application [5, 6]. The main characteristics of powders are particle size (granulometry) and particle shape (morphology). Technological properties of powders (bulk density, flowability, surface area, apparent density, etc.) as well as the potential areas of their applications depend on these characteristics [7].

The granulometry of powders can be determined by different methods (sieve analysis, image analysis, laser analysis, etc.) but adequate description of the powder granulometry by these methods still remains undetermined. However, some investigations showed [8] that the evaluation of coarse powder granulometry (particle size above 50 μm) by means of sieve analysis guarantees sufficiently good

V. M. Maksimović (✉)
Institute of Nuclear Sciences «Vinča», P.O. Box 522,
11001 Belgrade, Serbia
e-mail: vesnam@vinca.rs

Lj. J. Pavlović · M. G. Pavlović
ICTM, Institute of Electrochemistry, Njegoševa 12,
11000 Belgrade, Serbia

M. V. Tomić
Faculty of Technology Zvornik, University of Eastern Sarajevo,
75400 Zvornik, Republic of Srpska

results. Evaluation of the fine powder granulometry (with particle size less than 50 μm) is more difficult. The results of the sieve analysis do not adequately describe the powder granulometry. Sieving analysis is relatively time consuming and requires a complex set of sieves in different mesh sizes to achieve useful results. If the steps between the sieve classes are too large the information on particle size distribution of powders are limited or even useless [9]. The morphology of powder particles is characterized by description (spherical, angular, dendritic, dish-shaped, acicular), or quasi-quantitatively, for example, by means of geometric parameters. For characterization of real particles, the particle shape becomes more and more important in addition to particle size. Image analysis proved to be helpful in describing powder particles. The methods used to measure the powder particle size, also enabling the analysis of the particle size distribution, could be divided into two groups: direct [10] and indirect [10, 11]. The direct methods map the geometry of individual particles via light, electron scanning, and transmission microscopy. Indirect methods such as sieve and laser analysis are based on physical properties of powder.

Stereological methods could be used for precise description of powder based on their planar images. Useful for powder characterization are parameters measured for individual “objects” (projection of powder particle) such as: area, perimeter and roundness, a shape factor which gives a minimum value of unity for a circle. This is calculated from the ratio of the perimeter square to the area, as below:

$$f_R = \frac{L_p^2}{4\pi A \cdot 1.064} \quad (1)$$

where f_R is the *roundness* shape factor which gives a minimum value of unity for a circle; A is the *area* total number of detected pixels within the feature; L_p is the *perimeter*, the total length of the boundary of the feature, calculated from the horizontal and vertical projections, with an allowance for the number of corners. The adjustment factor of 1.064 corrects the perimeter for the effect of the corners produced by the digitalization of the image [12].

Pure copper powder is widely used in the electrical and the electronic industries because of its excellent electrical and thermal conductivities. Pure copper powder may be obtained for demands by electrodeposition. Electrodeposition has two stages, i.e., nucleation and growth. In the case of smooth cathodes, the growth process is enhanced through nucleation, but the growth process is dominant for powder production where each nucleus is a powder particle. Therefore, the obtainment of a proper particle size of the copper powder is strongly dependent on the relative rates of nucleation and crystal growth [4, 13].

Direct and indirect measurements of galvanostatically deposited copper powder particles were the objects of this article.

2 Experiment

Copper powders were galvanostatically deposited by applying magnitudes of current densities of $j = 7.71, 10.28, 12.85, 24, 30,$ and 36 A dm^{-2} . The experiments were performed in an enlarged laboratory reactor with a cell volume of 10 dm^3 . The electrolytic copper powders were produced from electrolyte containing 145 g dm^{-3} sulphuric acid and 18 g dm^{-3} copper (impurities: 0.4 mg dm^{-3} Pb, 4.5 mg dm^{-3} Fe, 5.6 mg dm^{-3} Ni, 0.1 mg dm^{-3} Zn), using an electrolyte temperature of $50 \pm 2 \text{ }^\circ\text{C}$. The electrolyte circulation system was designed to supply the laboratory scale cell from one electrolyte supply tank (100 dm^3). The enlarged laboratory reactor had a circulation pump, inlet and outlet for electrolyte, and heat exchanger. The latter controlled the electrolyte temperature. Electrolyte was pumped from a basement storage tank to the enlarged laboratory reactor (electrolyte rate $0.11 \text{ dm}^3 \text{ min}^{-1}$). From there it flowed by gravity and then into the back and top of the cell. Thus, circulation of electrolyte in the tanks was top to bottom. This yields a finer, more homogeneous powder than bottom to top circulation. Electrolyte returns to the basement storage by gravity. The cell was loaded with four copper cathodes at a spacing of 30 mm between center (each holding four vertical copper rods of 120-mm length and 8-mm diameter), and five copper anodes ($120 \times 120 \times 10$ mm which were suspended between the cathodes. The distance between anodes was 60 mm from center of each anode. The electrodes in the cell were parallel with each other [12, 14].

The electrolyte was prepared from technical grade chemicals and demineralized water. The wet powders were washed several times at room temperature with a large amount of demineralized water until the powders were free from traces of acid. In order to inhibit oxidation, benzoic acid, as a stabilizer, was added to (0.1%) to the water for washing copper powders, to protect the powders against subsequent oxidation. This substance was removed by further washing [14].

Granulometry and morphology studies of powders were carried out using four methods:

- sieve analysis [15]
- light microscopy, transmission method, to produce projections of powder particles,
- scanning electron microscopy (SEM)
- X-ray analysis.

The morphology of electrodeposited copper powders was examined using (SEM), PHILIPS, type XL30. Quantitative microstructural characterization of copper powders was performed using a Zeiss Axiovert 25 light microscope equipped with a digital camera Panasonic WV-CD50 and software Leica QWin for automatic image analysis.

X-ray powder diffraction (XRD) analysis of copper powders was carried out on a Simens D500 diffractometer with a Ni filter and CuK_α radiation operated at a tube voltage of 35 kV and a tube current of 20 mA. The experiments were performed in the diffraction angle range of $2\theta = 40\text{--}100^\circ$. From X-ray diffractograms, the crystallite sizes were calculated using the Scherrer formula [16, 17].

3 Results and discussion

3.1 SEM investigations of morphology

Dendritic morphology is a characteristic of all the copper powders obtained at constant current density. Typical dendritic particles of copper powder are shown in Fig. 1. Careful analysis of the microphotographs shows that with increased current density the morphology of copper powder particles is changed from compact, massive dendrites (Fig. 1a) and massive particles (designated in Fig. 1b with number 1) to branched 3D dendrites [18, 19] (designated in Fig. 1b with number 2) as well as in Fig. 1c and d.

In powder samples formed at lower current density ($j = 7.71$ and 10.28 A dm^{-2}) both dendrite types were observed: massive dendrites with the secondary dendritic branches defined with the low-energy facets [20], as well as branched 3D dendrites. With increased current density $j = 30 \text{ A dm}^{-2}$ and $j = 36 \text{ A dm}^{-2}$ massive dendrites disappeared.

Further careful analysis of the surface morphologies (Fig. 2a–g) indicated that with an increase of the current density, the surface morphology was significantly changed.

At a current density of $j = 7.71$ and $j = 10.28 \text{ A dm}^{-2}$ (Fig. 2a, b and c, d) very rough and jagged polycrystalline faces are observed which are ideal for creation of new nucleuses and crystal growth (mixed activation–diffusion control). Some dendritic branches of massive dendrites are defined by the flat cubic {100} and octahedral {111} faces (Fig. 2b). The final shape of crystals is determined by planes with lower growth velocities [19]. With increased current density, the possibility for diffusion control is increased, and particles become more dendritic, acquiring a corn-like shape (Fig. 2e, f) which gives a fern-like structure (Fig. 2 g, h). Most probably, the tertiary branches grow out along the cube edges in the [100] direction (Fig. 2g, h).

3.2 Size and shape

Typical particle-size distributions for copper powders obtained at four different current densities are shown in Fig. 3a. On the other side, from Fig. 3b, it may be seen that the mean particle size decreases with increasing current density. Analysis of the presented results shows that over 50% of the mean particle size values are less than $50 \mu\text{m}$. Furthermore, the values of mean particle sizes based on a cumulative curve distribution (at the point 50%) are within a range of $52.90\text{--}73.63 \mu\text{m}$ (Fig. 3b). Insignificant deviation with single samples containing dendrites of small granulation can be explained with the unreliability of sieve analysis of the smaller granulation (below $50 \mu\text{m}$).

For the purpose of quantitative microscope analysis, the relevant parameters selected for describing copper powder particles [21–23] were area, perimeter, and roundness

Fig. 1 SEM microphotographs of copper powder particles deposited at current density:
a $j = 7.71 \text{ A dm}^{-2}$;
b $j = 10.28 \text{ A dm}^{-2}$;
c $j = 30 \text{ A dm}^{-2}$;
d $j = 36 \text{ A dm}^{-2}$

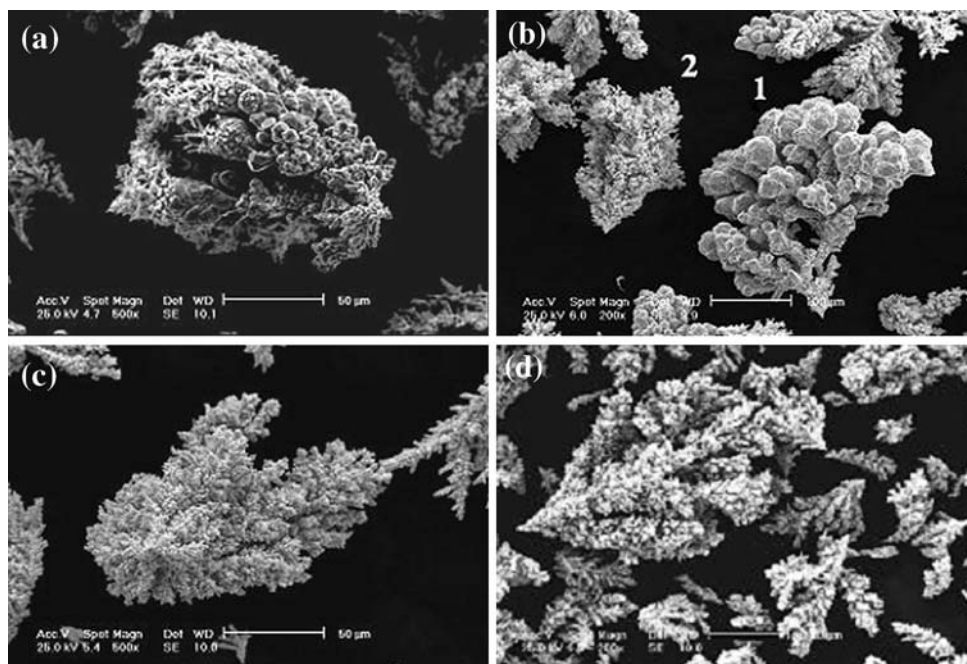
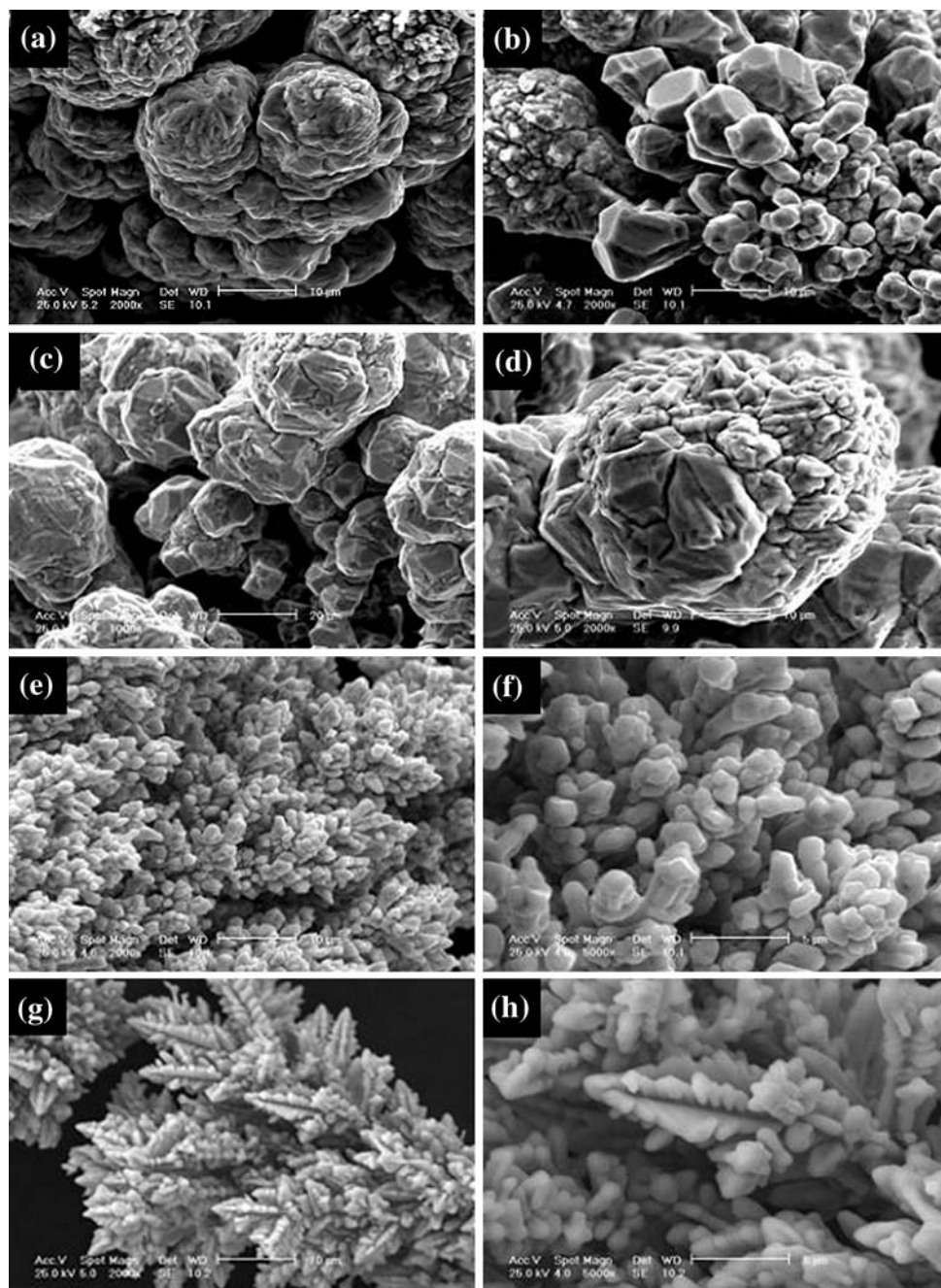


Fig. 2 Surface morphology of copper powder particles: **a, b** $j = 7.71 \text{ A dm}^{-2}$; **c, d** $j = 10.28 \text{ A dm}^{-2}$; **e, f** $j = 30 \text{ A dm}^{-2}$; **g, h** $j = 36 \text{ A dm}^{-2}$



(roundness is a shape factor which unites the area and the perimeter as stereological parameters of structure).

Applying this analysis, it was noticed that there were distinctly voluminous particles, especially at a lower current density. It was assumed that such particles were formed in conditions of deposition at the end of particle growth. At a higher magnification (Fig. 2), it is clear that the development of dendrites with fine dendritic branches starts at the voluminous particles.

The dependence of the total length of the particle boundary (perimeter), (Fig. 4) and the particle area, (Fig. 5a) shows a linear decreasing dependence on the

current density. The analysis of change of shape factor shows the same dependence (Fig. 5b), with a deviation which appears with a sample of copper powder deposited at $j = 10.28 \text{ A dm}^{-2}$ (large fraction) [7]. The changes of values of the area, the perimeter, and roundness with current density as well as the corresponding RSE (relative standard error of measurement) values are given in Table 1.

Dominant larger fractions with samples $j = 7.71 \text{ A dm}^{-2}$ and $j = 10.28 \text{ A dm}^{-2}$ dictate high area values and a high scattering of results. In general, with an increase of current density, a decrease of dendrites size occurs (low value of

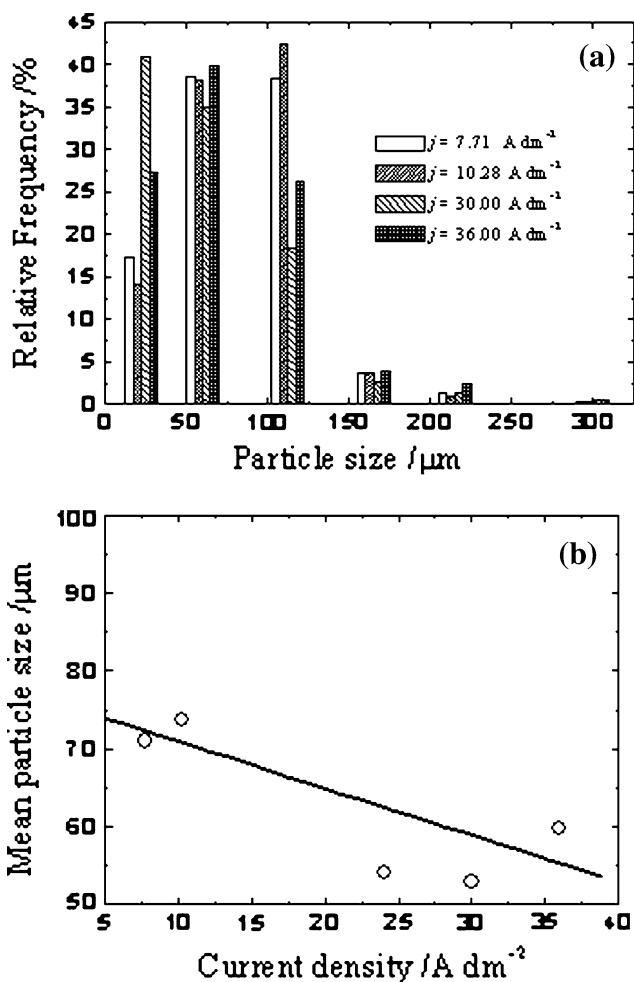


Fig. 3 a Particle size distribution of copper powders deposited by galvanostatic regime—histogram obtained by sieved analysis; b the effect of current density change on value of mean particle size

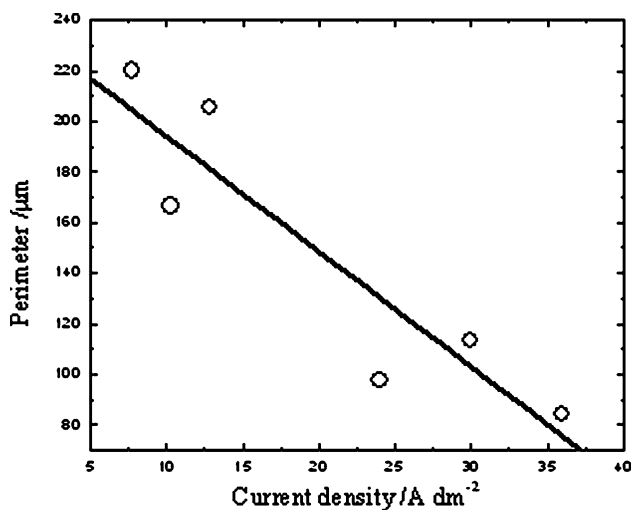


Fig. 4 The dependence of the perimeter on current density

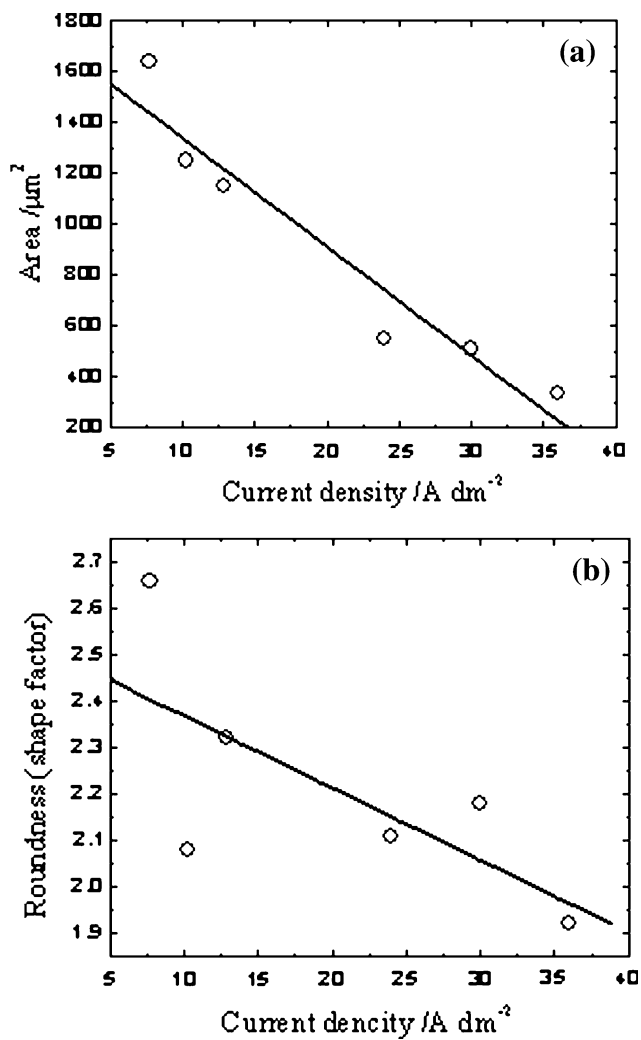


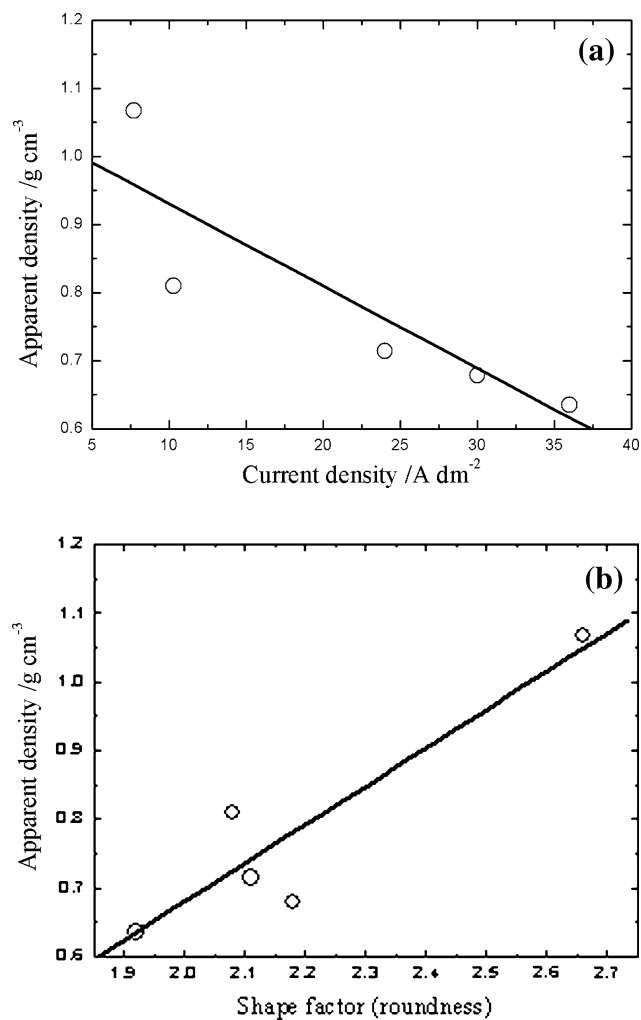
Fig. 5 The dependence of a the area and b the roundness on current density

the selected shape factor), Fig. 5b. The deviation that appeared in this analysis may be the result of the presence of dendrites of different morphologies in the same sample. The dependence of the apparent density (Fig. 6a) shows a linear decreasing dependence on current density while the apparent density increases with an increase of the shape factor, i.e., roundness (Fig. 6b).

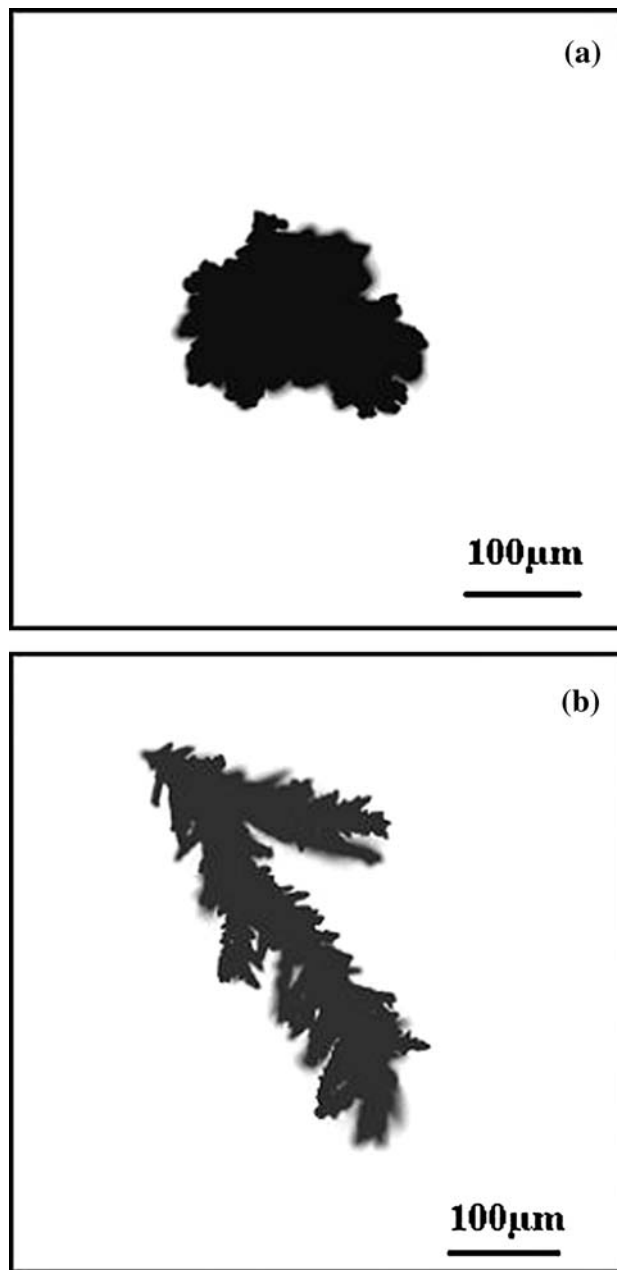
The shape factor i.e., roundness is an especially useful parameter when comparing morphologies of powders deposited at potentiostatical and galvanostatical regimes (Fig. 7), and the reverse current regime. With the powder samples obtained in the conditions of reverse current, the values of the changes of perimeter and area do not follow a linear dependence, as it is case with powders obtained at constant current density. Figure 7 shows a difference in shape of massive and branched dendrites. Image analysis indicated that massive dendrites have a high value of the area according to the total length of the boundary

Table 1 The change of values of the area, the perimeter, and roundness with current density at galvanostatic regime, as well as the corresponding RSE (relative standard error of measurement)

Current density (A dm^{-2})	7.71	10.28	12.85	24	30	36
Roundness	2.66	2.08	2.32	2.11	2.18	1.92
RSE (%)	6.70	4.94	16.4	6.77	3.41	2.29
Perimeter (μm)	220.13	166.55	205.30	97.84	113.13	84.19
RSE (%)	10.23	10.6	16.55	9.08	6.01	5.05
Area (μm^2)	1638.55	1249.91	1150.12	550.46	509.06	336.19
RSE (%)	14.76	14.89	17.45	13.86	7.98	8.26

**Fig. 6** The dependence of the apparent density **a** on current density and **b** on the roundness

(perimeter) in contrast to branched dendrites which have high values of perimeter according to the area. These differences are most visible if we observe the change of roundness. The mean value of shape factor, i.e., roundness of massive dendrites is 2.07, and for branched dendrites it is 7.13.

**Fig. 7** Samples of particles **a** massive dendrite deposited galvanostatically ($j = 20 \text{ A dm}^{-2}$); **b** branched dendrite deposited potentiostatically ($\eta = 700 \text{ mV}$)

In the case of deposition of powder at constant current, the apparent current density remains constant, but the real current density decreases due to an increased surface of the electrode. This results in a decrease of overpotential of the deposition. A higher decrease of deposition overpotential means the formation of dispersed deposits. With an increase of current density the process is carried out with greater diffusion difficulties provoked by numerous changes in copper powder characteristics together with a large number of new crystallization centers formed. These factors influence an increase of powder particles dispersity and their more dendritic structure. It leads to a reduction of particle size and apparent density and to enlargement of specific area [12].

3.3 X-ray analysis

X-ray diffractograms of four copper powders are reproduced in Fig. 8. Five sharp diffraction peaks were observed. Distinct diffraction peaks were observed at 2θ 43.412° (43.463°, 43.416° and 43.360°), 50.557° (50.574°, 50.550° and 50.470°), 74.232° (74.258°, 74.190° and 74.122°), 90.012° (90.024°, 89.938° and 89.930°), and 95.219° (95.231°, 95.199° and 95.149°), respectively, corresponding to (111), (200), (220), (311), and (222) crystalline planes of cubic Cu (JCPDC card No. 04-0836).

The average crystallite sizes, shown as a function of deposition current density in Fig. 9, were calculated using half width of the (111) peaks ($0.207^\circ < 2\Delta\theta > 0.380^\circ$) by the Scherrer formula. The results show that there exists a linear correlation between crystallite size and current

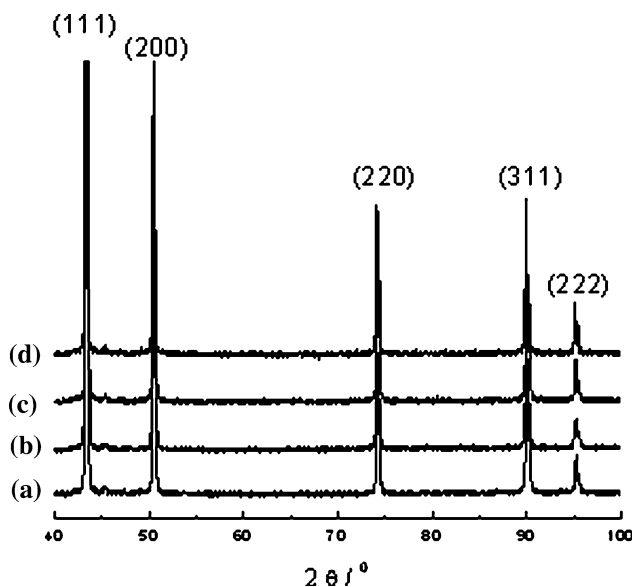


Fig. 8 X-ray diffraction patterns of copper powders deposited at (a) $j = 7.71 \text{ A dm}^{-2}$, (b) $j = 10.28 \text{ A dm}^{-2}$, (c) $j = 30 \text{ A dm}^{-2}$, and (d) $j = 36 \text{ A dm}^{-2}$

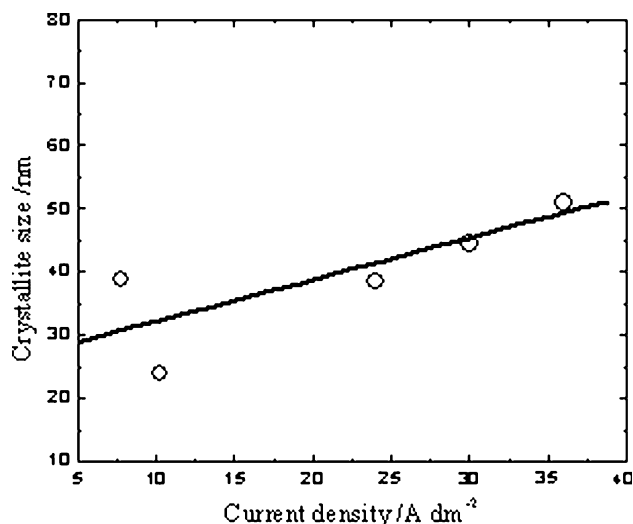


Fig. 9 The dependence of crystallite size on current density

density of deposition, which is a linear increasing dependence. During electrodeposition impurities may be incorporated into the crystal lattice [24], but in this case the presences of impurities from technical chemicals could not be the reason for such a dependence. With an increase of current density, a more intense incorporation of copper adatoms into the crystal lattice takes place, which results in an increase of crystallite size. This effect is much greater than the effect that impurities from the electrolytes have on both nucleation and growth of deposited powders.

4 Conclusion

The results of this article showed that with the an increase of current density the morphology of copper powder particles is changed from compact, massive dendrites to dispersed dendrites with corn-like and fern-like surfaces. At the same time, the mean particle size is decreased. All the selected parameters show a linear decreasing dependence of current density. The shape factor, i.e., roundness could be a useful parameter for describing morphology of powders deposited by different regimes. XRD analysis indicated that the crystallite sizes shows a linear increasing dependence on current density. With an increase of current density, a more intense incorporation copper of adatoms into crystal lattice takes place. The copper powders obtained by electrodeposition represent a dispersed deposit, which consists of particles of various forms and sizes, and so any one method alone is inadequate for characterization of powder particles.

Acknowledgment This study was financially supported by Ministry of Science of the Republic of Serbia under the research project: “Deposition of ultrafine powders of metals and alloys and

nanostructured surfaces by electrochemical techniques” (142032G/2006). The authors are indebted to Dr. Milan Jovanović for helpful discussion during the preparation of this article.

References

1. Industry Segment Profile SIC 33991 Metal powder production (2000) EPRI center for materials production
2. German RM (1994) Powder metallurgy science. Princeton, New Jersey
3. Despić A, Popov K (1972) Transport controlled deposition and dissolution of metals. In: Conway BE, Bockris JO'M (eds) Modern aspects of electrochemistry, vol 7. Plenum Press, New York
4. Nikolić ND, Pavlović LjJ, Pavlović MG, Popov KI (2008) Powder Technol 185:195
5. Popov KI, Pavlović MG (1973) Electrodeposition of metal powders with controlled particle grain size and morphology. In: White RW, Bockris JO'M, Conway BE (eds) Modern aspects of electrochemistry, vol 24. Plenum Press, New York
6. Pavlović MG, Popov KI (2005) Metal powder production by electrolysis In: Electrochemistry encyclopedia. Available via DIALOG. <http://electrochem.cwru.edu/ed/encycl/art-p04-metalpowder.htm>
7. Mikli V, Käerdi H, Kulu P, Besterce M (2001) Proc Estonian Acad Sci Eng 7:22
8. Kulu P, Tümanok A, Mikli V, Käerdi H, Kohutek I, Besterce M (1998) Proc Estonian Acad Sci Eng 4:3
9. Schmid H (2003) Metal powder report 58:26
10. Pons MN, Plagnieux V, Vivier H, Adet D (2005) Powder Technol 157:57
11. Michalski J, Wejrzanowski T, Pielaszek R, Konopka K, Lojkowski W, Kurzydłowski KJ (2005) Mater Sci (Poland) 23:79
12. Pavlović MG, Pavlović LjJ, Ivanović ER, Radmilović V, Popov KI (2001) J Serb Chem Soc 66:923
13. Xue J, Wu Q, Wang Z, Yi S (2006) Hydrometallurgy 82:154
14. Pavlović MG, Pavlović LjJ, Doroslovački ID, Nikolić ND (2004) Hydrometallurgy 73:155
15. ASTM B214-ISO 4497. Metallic powders; determination of particle size by dry sieving; test method for sieve analysis of granular metal powder
16. Ziegler G (1978) Powder Metall Int 10:70
17. Cullity BD (1967) Elements of X-ray diffraction. Addison-Wesley Publishing Company Inc, Ontario
18. Wranglen G (1960) Electrochim Acta 2:130
19. Maksimović VM, Pavlović MG, Pavlović LjJ, Tomić MV, Jović VD (2007) Hydrometallurgy 86:22
20. Sun Y, Xia Y (2002) Science 298:2176
21. De Hoff RT, Rhines FN (1968) Quantitative microscopy. McGraw Hill Book Comp, New York
22. Modin H, Modin S (1973) Metallurgical microscopy. Butterworths, London
23. Cvijović Z (1987) Ph.D. Thesis, University of Belgrade
24. Muresan LM, Varvara SC (2005) Leveling and brightening mechanisms in metal electrodeposition, Chap. 1. In: Nunez M (ed) Metal electrodeposition. Nova Science Publishers, New York